

## UNIFORM INDENTATION OF THE ELASTIC HALF-SPACE BY A RIGID RECTANGULAR PUNCH

P. W. BROTHERS

Department of Scientific and Industrial Research, Gracefield, New Zealand

G. B. SINCLAIR

Department of Mechanical Engineering, Carnegie–Mellon University, Pittsburgh, U.S.A.

and

C. M. SEGEDIN

School of Engineering, University of Auckland, Auckland, New Zealand

(Received 29 December 1976; revised 28 March 1977)

**Abstract**—The problem considered is that of a rigid flat-ended punch with rectangular contact area pressed into a linear elastic half-space to a uniform depth. Both the lubricated and adhesive cases are treated. The problem reduces to solving an integral equation (or equations) for the contact stresses. These stresses have a singular nature which is dealt with explicitly by a singularity-incorporating finite-element method. Values for the stiffness of the lubricated punch and the adhesive punch are determined: the effect of adhesion on the stiffness is found to be small, producing an increase of the order of 3%.

### INTRODUCTION

Contact problems in elasticity may be defined as problems associated with the determination of the distributions of stress and deformation throughout two elastic bodies which are pressed together. Such problems are of importance to the engineer in a wide range of design fields. Consequently they have attracted a wealth of investigations, the Russian literature being especially rich as is evidenced by Galin's book [1]. Reviews of the area are provided by Goodier in [2] and Lubkin in [3].

Most treatments of contact problems employ a host of simplifying assumptions in order to make the analysis tractable. The present paper is no exception. We restrict our considerations to *flat-ended rigid punches* which are pressed into the *linear elastic half-space* to a *uniform depth*. Furthermore we assume that the contact surface is either *lubricated* (no resistance to slip) or *adhesive* (slip completely restrained).

This class of contact problems may be reduced to the solution of integral equations for the contact stresses. For some contact regions, such as the infinite strip or the ellipse, exact solutions of the integral equations are available. All these solutions feature *singularities in the contact stresses* at the edges of the punches. Thus for the punch we are particularly concerned with here—the punch with a *rectangular contact region*—we can expect the same sort of singular stress behaviour. Although singular stresses cannot occur in the real world situation modelled by these contact problems, they are a real aspect of this class of mathematical model and must be accommodated in any numerical approach if convergence is to be ensured.

Gorbunov-Possadov has devised one method for numerically evaluating the contact stress under a lubricated rectangular punch. The method, described in [4], approximates the contact stress distribution by a *truncated, double power series* and specializes the integral equation at a set of points to generate a sufficient system of linear equations for the series coefficients. A second method for the lubricated rectangular punch is contained in the work of Conway and Farnham [5].† This is a *direct finite-element method* wherein the area under the punch is divided into a number of elements over each of which the stress is assumed constant, and the integral equation specialized to generate a system of equations for these constants. Neither of these methods makes allowances for singular behaviour in the contact stress.

Borodachev and Galin [9] furnish a method which does allow to some extent for a stress

†Within the context of contact problems involving rigid punches, this direct finite-element method was apparently first used by Conway, Vogel, Farnham and So [6] to analyse indented slabs. It has subsequently been used on a number of related rigid-punch problems by Conway and his co-workers—see [7, 8] and Ref. in [5].

singularity in the lubricated rectangular punch problem. The method introduces the *singularity associated with the lubricated, infinite strip problem* and represents the contact stress distribution for the rectangular punch with square-root edge singularities across its width and Chebyshev polynomials along its length. Consequently the method is best suited to rectangles with large aspect ratios. The aim of the present paper is to extend this type of approach to rectangles of any aspect ratio: we do this with a *singularity-incorporating finite-element method* (hereafter referred to as the singularity method).

The singularity method is described in Section 1 through an application to the lubricated, infinite strip problem. Comparison with the exact solution for the problem affords an appraisal of the method and demonstrates that it has superior accuracy to the methods of Gorbunov-Possadov and of Conway *et al.*

Section 2 presents an application of the singularity method to the lubricated, rectangular punch problem. No analytical solution is available for this problem but some analytical bounds on the stiffness do exist (a derivation for two of the bounds is given in the Appendix). The values found for the stiffness are shown to satisfy these bounds.

Finally, in Section 3, the effects of adhesion are investigated and the singularity method applied to the adhesive rectangular punch. The results show that adhesion has little effect on stiffness, typically increasing it by 3%.

### 1. THE LUBRICATED INFINITE STRIP

In this section we consider the uniform indentation of the elastic half-space by a lubricated infinite strip. We formulate the problem within the context of two-dimensional elasticity theory and derive the associated integral equation. We then describe the application of our singularity method and compare the results obtained with the exact solution and with those obtained by the methods of Gorbunov-Possadov and of Conway *et al.*

To formulate the problem we let  $(x, y, z)$  be rectangular cartesian coordinates with origin 0 such that the surface of the half-space  $\mathcal{H}$  is formed by the  $xy$ -plane with  $z$  positive into the half-space. That is

$$\mathcal{H} = \{(x, y, z) \mid -\infty < x < \infty, -\infty < y < \infty, 0 < z < \infty\}. \quad (1.1)$$

The rigid punch indenting the half-space is in contact on  $\partial_1\mathcal{H}$ , an infinite strip of width  $2a$  centred on the  $y$ -axis. Consequently, if  $\partial_2\mathcal{H}$  is the region outside the punch, we have

$$\begin{aligned} \partial_1\mathcal{H} &= \{(x, y, z) \mid -a < x < a, -\infty < y < \infty, z = 0\}, \\ \partial_2\mathcal{H} &= \{(x, y, z) \mid a < |x| < \infty, -\infty < y < \infty, z = 0\}. \end{aligned} \quad (1.2)$$

The punch is pushed into the half-space, to a uniform depth  $d$  in the  $z$ -direction, by a load per unit length of  $P$  (Fig. 1).

For the infinite strip, the plane-strain simplification is appropriate (*viz.*  $\partial/\partial y$  a null operator and zero displacement in the  $y$ -direction). Accordingly, in the absence of body forces, the *equilibrium conditions* are

$$\frac{\partial\sigma_x}{\partial x} + \frac{\partial\tau_{zx}}{\partial z} = 0, \quad \frac{\partial\sigma_z}{\partial z} + \frac{\partial\tau_{zx}}{\partial x} = 0, \quad (1.3)$$

on  $\mathcal{H}$ . Here  $\sigma_x = \sigma_x(x, z)$ ,  $\sigma_z = \sigma_z(x, z)$  and  $\tau_{zx} = \tau_{zx}(x, z)$  denote the normal and shear stress components in the usual way.

The half-space is composed of a linear elastic material which is both homogeneous and isotropic. Thus the *stress-displacement relations* are

$$\sigma_x = \frac{2\mu}{(1-2\nu)} \left[ (1-\nu) \frac{\partial u}{\partial x} + \nu \frac{\partial w}{\partial z} \right], \quad \sigma_z = \frac{2\mu}{(1-2\nu)} \left[ \nu \frac{\partial u}{\partial x} + (1-\nu) \frac{\partial w}{\partial z} \right], \quad \tau_{zx} = \mu \left[ \frac{\partial u}{\partial z} + \frac{\partial w}{\partial x} \right], \quad (1.4)$$

on  $\mathcal{H}$ , where  $\mu$  is the shear modulus,  $\nu$  Poisson's ratio and  $u = u(x, z)$ ,  $w = w(x, z)$  the components of displacement in the  $x$ -,  $z$ -directions, respectively.

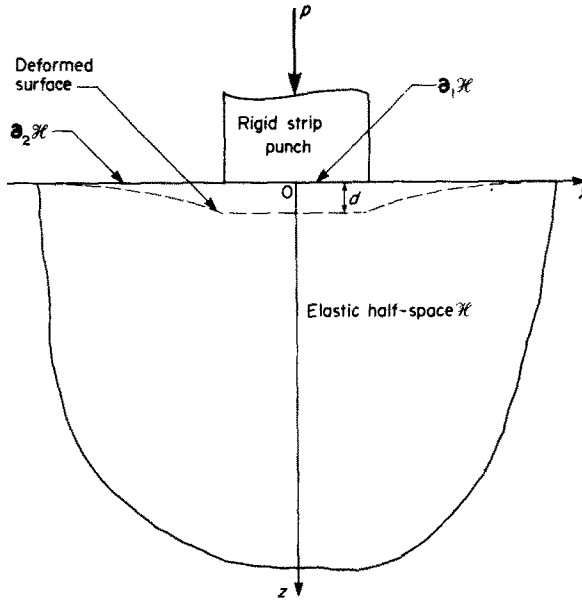


Fig. 1. Geometry and coordinates for the infinite strip.

The rigid punch is flat-ended and assumed to be lubricated, or smooth, so that there are no shear stresses under the punch. The surface of the half-space is stress-free outside the punch. Hence the *boundary conditions* are

$$\begin{aligned} w = d, \quad \tau_{zx} = 0 \quad \text{on } \partial_1 \mathcal{H}, \\ \sigma_z = \tau_{zx} = 0 \quad \text{on } \partial_2 \mathcal{H}. \end{aligned} \tag{1.5}$$

The appropriate *regularity requirements* at infinity and at the punch edges are

$$\begin{aligned} \sigma_x = o(1), \quad \sigma_z = o(1), \quad \tau_{zx} = o(1) \quad \text{as } r \rightarrow \infty, \\ \left. \begin{aligned} u = O(1), \quad w = O(1), \\ \sigma_x = O(r^{-\delta}), \quad \sigma_z = O(r^{-\delta}), \quad \tau_{zx} = O(r^{-\delta}) \end{aligned} \right\} \text{ as } r \rightarrow 0 (\delta < 1), \end{aligned} \tag{1.6}$$

on  $\mathcal{H}$ . Here  $r$  is the distance from either of the punch edges and  $\delta$  is a constant. Finally we have the *loading requirement*,

$$\int_{-a}^a \sigma_z(x, 0) dx = -P, \tag{1.7}$$

where the load  $P$  is taken to be positive for an indenting punch. Observe that the last of (1.6) ensures the convergence of the integral in (1.7).

The displacement field satisfying the preceding formulation is only unique to within a rigid-body translation in the  $z$ -direction.† This indeterminacy would be removed if we could exchange the first of (1.6) for a requirement that the displacements vanish at infinity. Unfortunately the problem so formulated has no solution. Thus the indeterminacy in the depth of indentation must be admitted, and we must include a loading requirement to ensure a non-trivial stress field.

We now reduce the problem to an *integral equation*. This reduction is accomplished by the superposition of the Flamant solution for a line-load.

For a line-load applied normal to the surface of the half-space  $\mathcal{H}$ , the *Flamant solution* has

†See Knowles and Sternberg[10], p. 1177 for an outline of a uniqueness proof.

the following properties: satisfaction of the plane-strain equations of elasticity on  $\mathcal{H}$ ; zero shear stress on the surface of  $\mathcal{H}$ ; zero normal stress on the surface of  $\mathcal{H}$  away from the line of application; and vanishing stresses at infinity. Consequently the superposition of such line-loads on the strip  $\partial_1\mathcal{H}$  will automatically satisfy the requirements set down in our formulation of the strip problem except for: the displacement boundary condition of (1.5); the regularity requirements at the punch edges of (1.6); and the loading requirement (1.7).

Turning to the first of these outstanding conditions, we draw on the Flamant solution for the surface displacement in the  $z$ -direction resulting from a normal surface line-load applied parallel to the  $y$ -axis and a distance  $\xi$  from it,

$$w = -\frac{1-\nu}{\mu\pi}F \ln \left| \frac{x-\xi}{a} \right| \quad (-\infty < x < \infty, -\infty < \xi < \infty, x \neq \xi). \tag{1.8}$$

In (1.8),  $F$  is the strength of the line-load (dimensions force/length) and  $w$  is arbitrary to the extent of a rigid-body translation—without loss of generality we take this rigid-body translation to be  $((1-\nu)/\mu\pi)F \ln a$ . Replacing the strength  $F$  in (1.8) by the “loadette”  $p(\xi) d\xi$ , and integrating with respect to  $\xi$  from  $-a$  to  $a$ , yields the surface displacement in the  $z$ -direction due to the contact stress  $p$  (positive for an indenting punch). Substituting into the first of (1.5) then gives

$$-\frac{1-\nu}{\mu\pi} \int_{-a}^a p(\xi) \ln \left| \frac{x-\xi}{a} \right| d\xi = d \quad (-a < x < a). \tag{1.9}$$

If we determine  $p$  such that (1.9) holds, the displacement boundary condition will be met.

From the forms for the stress and displacement fields in the Flamant solution it can be shown that the regularity requirements at the punch edges will be met provided the integral in (1.9) is convergent.

With respect to the loading requirement, recall that it was introduced to preclude a null stress field resulting for the strip problem, this possibility arising from the indeterminacy in  $d$  in (1.5). Observe that this indeterminacy has now been removed by our specific choice of the arbitrary rigid-body translation in (1.8). Consequently the loading requirement is no longer needed as such, and the strip problem has effectively been reduced to the determination of the contact stress  $p$  satisfying (1.9).

To simplify the problem further we introduce the dimensionless variables  $\bar{x} = x/a$ ,  $\bar{\xi} = \xi/a$  and  $\bar{p} = pa\bar{P}/P$ ,† where  $\bar{P}$  is a dimensionless load factor, and set  $d = (1-\nu)P/(\mu\pi\bar{P})$ . Thus we seek the dimensionless contact stress  $\bar{p}$  such that

$$-\int_{-1}^1 \bar{p}(\bar{\xi}) \ln |\bar{x} - \bar{\xi}| d\bar{\xi} = 1 \quad (-1 < \bar{x} < 1). \tag{1.10}$$

The exact solution of (1.10) is well-known‡ and we merely cite the result together with that for  $\bar{P}$  derived from (1.7):

$$\bar{p} = 1/(\pi\sqrt{(1-\bar{x}^2)} \ln 2) \quad (-1 < \bar{x} < 1), \quad \bar{P} = 1/\ln 2. \tag{1.11}$$

Equations (1.11) serve to evaluate the accuracy of our singularity method when applied to the strip.

In applying the singularity method to the integral eqn (1.10), we focus on the two singularities in the integrand: the square-root singularity in  $\bar{p}$ —the *stress singularity*; and the logarithmic singularity arising from the superposition of line-loads—the *superposition singularity*. We treat the stress singularity analytically and the superposition singularity with a singularity programming technique.

†Here, and henceforth, a bar indicates a quantity that has been rendered dimensionless.

‡See, for example, Muskhelishvili[11], p. 480.

Since we know that the contact stress in the strip problem has square-root singularities at the punch edges, we incorporate this feature directly, setting

$$\bar{p}(\bar{\xi}) = \frac{\bar{q}(\bar{\xi})}{\sqrt{(1-\bar{\xi}^2)}} \quad (-1 < \bar{\xi} < 1) \tag{1.12}$$

in (1.10), where  $\bar{q}$  is the *regular stress*. The explicit square-root singularity introduced into (1.10) via (1.12) is removed by the change of variable  $\bar{\xi} = \sin \phi$ , with  $\bar{x} = \sin \Phi$  and  $\bar{q}(\bar{\xi}) = \bar{q}(\phi)$ , to give

$$-\int_{-\pi/2}^{\pi/2} \bar{q}(\phi) \ln |\sin \Phi - \sin \phi| d\phi = 1 \quad (-\pi/2 < \Phi < \pi/2). \tag{1.13}$$

The solution is performed by a finite-element technique. The interval of integration is divided into  $2n$  equal elements, over each of which the regular stress  $\bar{q}$  is assumed constant; *i.e.*  $\bar{q} = \bar{q}_i$  on  $E_i = \{\phi | -\pi(n+1-i)/2n < \phi < -\pi(n-i)/2n\}$ , the  $i$ th element, for  $i = 1, 2, \dots, 2n$ . Hence (1.13) becomes

$$-\sum_{i=1}^{2n} \bar{q}_i \int_{E_i} \ln |\sin \Phi - \sin \phi| d\phi = 1 \quad (-\pi/2 < \Phi < \pi/2). \tag{1.14}$$

The symmetry of the regular stress reduces the number of unknowns in (1.14) to  $n$ , and taking the  $n$  values of  $\Phi$  associated with the mid-points of the elements  $E_n, E_{n+1}, \dots, E_{2n}$  generates a sufficient set of equations for the determination of  $\bar{q}_i$ .

Although the *coefficient integrals* in (1.14) can be evaluated analytically, the analogous terms in an application of the singularity method to the rectangular punch cannot. Since the main aim of this section is to evaluate the singularity method with a view to its eventual application to the rectangular punch, we disregard the analytical equivalents of the coefficient integrals and handle them numerically.

Notice therefore, that though we have dealt with the stress singularity exactly, we are still faced with the treatment of the superposition singularity. Away from  $\phi = \Phi$  the mid-ordinate rule suffices to calculate the coefficient integrals: but near  $\phi = \Phi$  the logarithmic superposition singularity makes its presence felt and we need an approach that recognizes it. We choose to deal with the difficulty by means of a singularity programming technique because this kind of technique has been shown to have a high computational efficiency.†

The ideas underlying our *singularity programming* technique are as follows. We assume that, if  $I$  is the integrand containing the singularity, we can write

$$I = I_r + I_s, \tag{1.15}$$

on the interval of integration, where  $I_r$  is regular and continuous and  $I_s$  has the singular character. We obtain  $I_s$  by finding the asymptotic behaviour of  $I$  near the singularity and require that  $I_s$  can be integrated analytically. Then, if  $\Delta$  denotes our normal quadrature formula, we have

$$\int I = \int I_r + \int I_s \doteq \Delta I_r + \int I_s, \tag{1.16}$$

because the regularity of  $I_r$  implies that  $\int I_r$  is well-approximated by the quadrature formula. From (1.15), we can replace  $\Delta I_r$  in (1.16) by  $\Delta I - \Delta I_s$  to obtain

$$\int I \doteq \Delta I + \int I_s - \Delta I_s. \tag{1.17}$$

†See Emery and Segedin[12].

The first term on the right-hand side of (1.17) represents the original approximation for  $f I$ ; the second term,  $f I_s - \Delta I_s$ , can be interpreted as a *correction term*.

For the present problem  $I = \ln |\sin \Phi - \sin \phi|$ —see (1.14). Thus setting  $\phi = \Phi + \epsilon$  and expanding  $I$  in terms of  $\epsilon$  gives

$$I_s = \ln |\epsilon \cos \Phi| + O(\epsilon) \quad \text{as } \epsilon \rightarrow 0 (-\pi/2 < \Phi < \pi/2). \quad (1.18)$$

Analytical integration of  $I_s$  is elementary and accordingly we may employ our singularity programming technique.

Applying (1.17) to (1.14) using (1.18), we find that the correction term decays quite rapidly away from the element containing  $\Phi$ , but contributes significantly near this element. The coefficient integrals so computed combine to produce a coefficient matrix which is neither symmetric nor sparse, but is well-conditioned and amenable to solution by the Crout reduction method.

An appraisal of our singularity method requires an evaluation of how well it determines the contact stress *distribution*. To this end we compare two measures of the distribution:  $\bar{P}$ , the load factor, a measure of the average value; and  $\bar{M}$ , the second moment of the distribution, a measure of dispersion.† By definition and from (1.11),

$$\bar{M} = \int_{-1}^1 \bar{x}^2 \bar{p}(\bar{x}) d\bar{x} = 1/\ln 4. \quad (1.19)$$

The results found for  $\bar{q}_i$  can be processed to provide estimates of  $\bar{P}$  and  $\bar{M}$  which, when compared with exact values of (1.11), (1.19), enable calculation of the absolute percentage errors,  $e_p$ ,  $e_m$ , respectively. Figure 2 presents  $e_p$  and  $e_m$  for varying  $n$ , the number of *degrees of freedom* used in the singularity method (that is, the number of elements on the half-strip).

Also plotted in Fig. 2 are the errors for the methods of Gorbunov-Possadov ( $n$  equal to the number of terms in the power series) and of Conway *et al.* ( $n$  as for the singularity method). For all  $n$  shown, the error in the load factor,  $e_p$ , is significantly lower for the singularity method and this relative advantage is even more pronounced for the error in the second moment of the contact stress distribution,  $e_m$ .‡

To better quantify the discussion of the errors we model the error distribution with

$$e = A/n^c, \quad (1.20)$$

where  $e$  is either of the errors  $e_p$ ,  $e_m$ ;  $A$  can be interpreted as an *accuracy parameter*; and  $c$  is a measure of the *convergence rate*. Fitting (1.20) to the curves in Fig. 2 gives an excellent match and thereby justifies (1.20) as an error model (provided  $n \geq 10$  for Gorbunov-Possadov's method, the correlation coefficients for all three methods are in excess of 0.999 in absolute value). Table 1 exhibits the results for  $A$  and  $c$ .

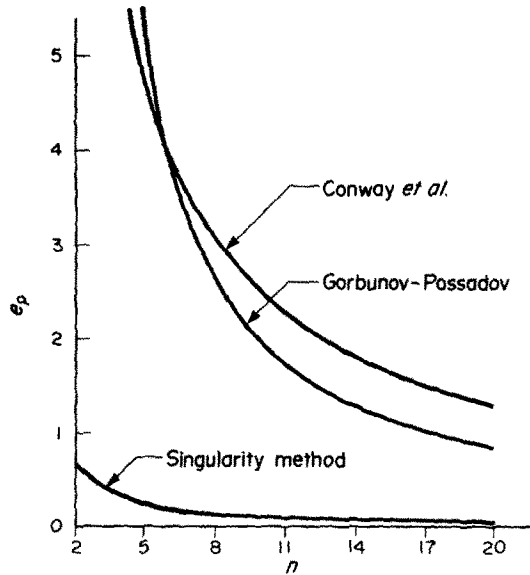
Although the convergence rates in Table 1 are quite similar for all three methods, the accuracy of the singularity method is superior as is reflected by its lower  $A$ -values. For the  $\bar{P}$ -determination,  $A$  is at least a factor 15 smaller for the singularity method and the superiority

Table 1. Comparison of accuracies and convergence rates

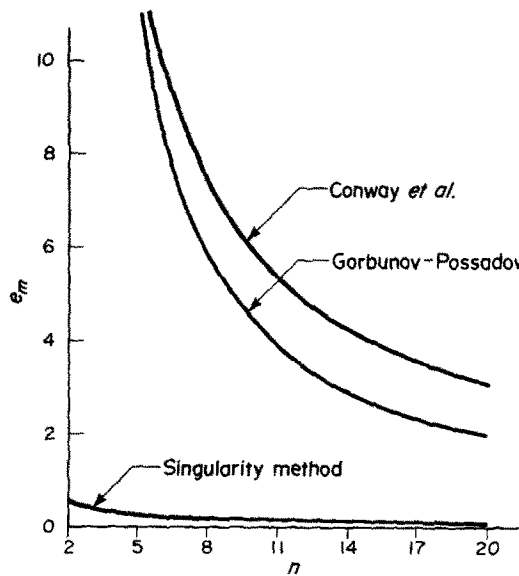
Method	For $e_p$		For $e_m$	
	$A$	$c$	$A$	$c$
Gorbunov-Possadov ( $n \geq 10$ )	32.9	1.23	66.9	1.19
Conway <i>et al.</i>	22.5	0.96	53.8	0.96
Singularity method	1.5	1.13	1.0	1.00

†Note that a statistic such as a  $\chi^2$  variable taken along some sub-interval of  $(-1 < \bar{x} < 1)$  has an unstable dependence on the proximity of its end-points to  $\pm 1$ .

‡Improvements to the methods of Gorbunov-Possadov and of Conway *et al.* suggest themselves. These include higher-order elements (effectively a combination of the two methods) and mesh refinement. For the infinite strip problem, varying degrees of mesh refinement for constant and cubic elements were investigated. In all instances, the errors  $e_p$ ,  $e_m$  for the singularity method were found to be lower.



(a)



(b)

Fig. 2. Errors in  $\bar{P}$  and  $\bar{M}$  for the infinite strip.

so indicated is increased for the  $\bar{M}$ -determination wherein  $A$  is at least a factor of 50 smaller. Table 1 thus demonstrates the advantage of taking the stress singularity into account.

Finally it is worth noting that, in the application of Gorbunov-Possadov's method in [4] to the three-dimensional problem of the rectangular punch, the number of degrees of freedom used corresponds to an  $n$  of 5 here. Similarly, Conway and Farnham in [5] use what corresponds to an  $n$  of 5. For  $n = 5$  the errors in these methods are  $e_p = 5.2, 4.8$  and  $e_m = 10.8, 11.5$ , respectively. The errors in the singularity method at  $n = 5$  are  $e_p = e_m = 0.2$ .

In the next section we extend the ideas underlying the singularity method to a three-dimensional problem.

## 2. THE LUBRICATED RECTANGULAR PUNCH

We now treat the problem of the uniform indentation of the elastic half-space by a lubricated rectangular punch. We describe the application of the singularity method and then present the results together with some analytical bounds.

To formulate the problem we take  $\mathcal{H}$  to be the half-space as previously, and subdivide its surface into a *rectangular contact region*  $\partial_1\mathcal{H}$  and a region outside the punch  $\partial_2\mathcal{H}$ . The rectangular contact region is centred on the origin 0 and has sides  $2a$ ,  $2b$  parallel to the  $x$ -,  $y$ -axes, respectively. Thus

$$\begin{aligned} \partial_1\mathcal{H} &= \{(x, y, z) \mid -a < x < a, -b < y < b, z = 0\}, \\ \partial_2\mathcal{H} &= \{(x, y, z) \mid a < |x| < \infty, b < |y| < \infty, z = 0\}. \end{aligned} \tag{2.1}$$

The punch is pushed into the half-space, to a uniform depth  $d$ , by a *total load*  $P$  (Fig. 3).

The problem is *three-dimensional*. Consequently we have the six components of stress  $\sigma_x, \sigma_y, \sigma_z, \tau_{xy}, \tau_{yz}, \tau_{zx}$ , where  $\sigma_x = \sigma_x(x, y, z)$ , etc. denote the normal and shear stresses in the usual way, and the three components of displacement  $u, v, w$  in the  $x$ -,  $y$ -,  $z$ -directions. The appropriate *field equations* on  $\mathcal{H}$  are the standard, three-dimensional, stress equations of equilibrium and stress-displacement relations, *viz.* the three-dimensional versions of (1.3), (1.4).

The rigid rectangular punch is flat-ended and lubricated. The surface of the half-space is stress-free outside the punch. Hence the *boundary conditions* are

$$\begin{aligned} w = d, \quad \tau_{yz} = \tau_{zx} = 0 \quad \text{on } \partial_1\mathcal{H}, \\ \sigma_z = \tau_{yz} = \tau_{zx} = 0 \quad \text{on } \partial_2\mathcal{H}. \end{aligned} \tag{2.2}$$

To complete our formulation we have the *regularity requirements* which insist that the displacements vanish at infinity (thereby exempting a loading requirement) and that the contact stresses be integrable over the punch-end with the displacements bounded there.

The derivation of the associated *integral equation* for the problem is achieved by the superposition of the *Boussinesq solution* for a normal point-load on the elastic half-space. The properties of the Boussinesq solution reduce the problem to the determination of the *contact stress*  $p$  (positive for an indenting punch) satisfying

$$\frac{1-\nu}{2\mu\pi} \int_{-b}^b \int_{-a}^a \frac{p(\xi, \eta)}{\sqrt{[(x-\xi)^2 + (y-\eta)^2]}} d\xi d\eta = d(-a < x < a, -b < y < b). \tag{2.3}$$

Equation (2.3) is simplified by the introduction of dimensionless variables:  $\bar{x}, \bar{\xi}$  as defined earlier; their counterparts  $\bar{y} = y/b, \bar{\eta} = \eta/b$ ;  $\alpha = b/a$ , the *aspect ratio* of the punch; and

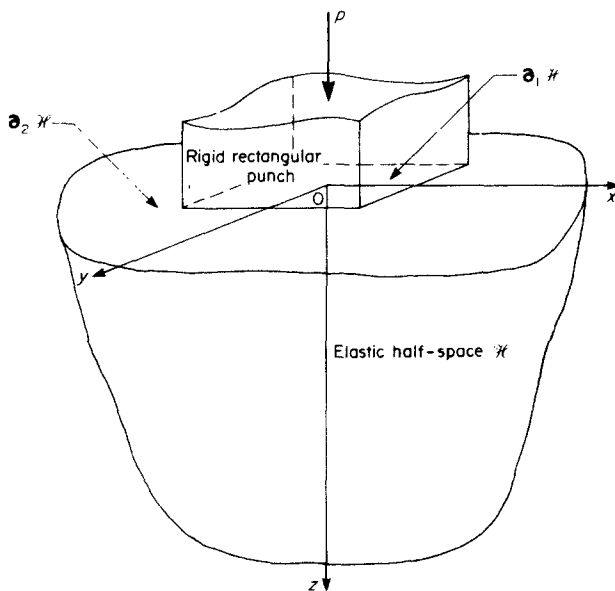


Fig. 3. Geometry and coordinates for the rectangular punch.



$\bar{p} = pabk/(\pi P)$ , where  $k$  is a *dimensionless punch stiffness*,

$$k = \frac{1 - \nu P}{2a\mu d} = \pi \int_{-1}^1 \int_{-1}^1 \bar{p}(\bar{x}, \bar{y}) d\bar{x} d\bar{y}. \quad (2.4)$$

It then becomes

$$\int_{-1}^1 \int_{-1}^1 \frac{\bar{p}(\bar{\xi}, \bar{\eta})}{\sqrt{[(\bar{x} - \bar{\xi})^2 + \alpha^2(\bar{y} - \bar{\eta})^2]}} d\bar{\xi} d\bar{\eta} = 1 \quad (-1 < \bar{x} < 1, -1 < \bar{y} < 1). \quad (2.5)$$

Following the pattern of development for our singularity method in Section 1, we now seek to incorporate the stress singularity in  $\bar{p}$  directly. Unfortunately the exact singular character of  $\bar{p}$  is not known. Nevertheless we can assess its singular character to some extent from related problems. The infinite strip problem described in Section 1 contains square-root stress singularities at its edges. This suggests that the rectangular punch may have square-root stress singularities at its edges *away from the corners*. The uniform indentation of the elastic half-space by a lubricated flat-ended punch which is in contact over an infinite wedge is analysed by Rvachev in [13]. For a wedge vertex angle of  $\pi/2$ , he shows that the asymptotic behaviour of the contact stress  $p$  in the corner can be expressed by

$$\begin{aligned} p &= \text{ord}(r^{-0.686}) \text{ as } r \rightarrow 0 \quad (-\pi/4 < \theta < \pi/4, \theta \text{ constant}), \\ p &= \text{ord}(1/\sqrt{[(\pi/4)^2 - \theta^2]}) \text{ as } \theta \rightarrow \pm \pi/4 \quad (r > 0, r \text{ constant}), \end{aligned} \quad (2.6)$$

where  $(r, \theta)$  are polar coordinates with  $r = 0$  at the wedge vertex and the line  $\theta = 0$  bisecting the wedge.† Taking into account this *possible* singular nature *near the corners*, together with that suggested for away from the corners, leads us to set

$$\bar{p}(\bar{\xi}, \bar{\eta}) = \frac{\bar{q}(\bar{\xi}, \bar{\eta})}{\sqrt{[(1 - \bar{\xi}^2)(1 - \bar{\eta}^2)]}} \quad (-1 < \bar{\xi} < 1, -1 < \bar{\eta} < 1) \quad (2.7)$$

in (2.5), where  $\bar{q}$  is the *regular stress*.

Observe that the form in (2.7) can admit an inverse-distance singularity as the corner is approached—a stronger singularity than that found by Rvachev for the corresponding wedge problem. Such “overestimating” of singular character merely means that, if the singular character in the corners of the rectangular punch is actually the same as in (2.6), then  $\bar{q}$  will tend to zero there. This in no way conflicts with our objective of ensuring that  $\bar{q}$  is regular (or continuous) in order that its numerical evaluation will converge rapidly. However, if the form in (2.7) is an “underestimate” of the actual singular character in the rectangular punch problem, then  $\bar{q}$  will not be “regular” and we may encounter difficulties in its numerical evaluation. At present we cannot guarantee that  $\bar{q}$  of (2.7) will in fact be regular: ultimately the vindication of the choice of (2.7) rests with the numerical results achieved using it.

A further factor influencing the choice of the form in (2.7) is that the singularity so introduced into (2.5) can be removed by a change of variable analogous to that of Section 1, namely  $\bar{\xi} = \sin \phi$ ,  $\bar{\eta} = \sin \psi$ . Thereafter the numerical evaluation of  $\bar{q}$  proceeds as previously. That is,  $\bar{q}$  is approximated by a set of constants on rectangular elements and the integral equation specialized for a set of points sufficient to generate a system of equations for these constants, the symmetry of the problem being exploited. The coefficient integrals in the system are found numerically with the aid of our singularity programming technique for elements feeling the effects of the superposition singularity. The system is then solved numerically using the Crout method.

The results of  $\bar{q}$  justify the choice of (2.7) to incorporate the stress singularity. The rates of change of  $\bar{q}$  in the vicinity of the punch edges away from the corners are small and similar to

†Galín's analysis of the same problem, [1], Section 2.11, shows  $p = \text{ord}(r^{-1})$  as  $r \rightarrow 0$  ( $-\pi/4 < \theta < \pi/4$ ,  $\theta$  constant), but it contains an extraneous line-load on the surface of the half-space outside the punch.

those found in the interior of the punch where we expect the contact stress to be continuous, and  $\bar{q}$  tends to zero in the corners of the punch indicating a degree of overestimation there. As the stress singularity appears to be well-accommodated by (2.7), we anticipate good numerical convergence. This is indeed found to be the case with the changes in  $\bar{q}$  being uniformly less than 2% when the number of elements in the rectangle is increased from 64 to 256.

The values of the contact stress, determined on the conversion of  $\bar{q}$  via (2.7), comprise our solution for the lubricated rectangular punch problem. In the interests of brevity we summarize these results by giving the associated values for the stiffness  $k$  here; details of the contact stress distribution are given in [14].† From the second expression for  $k$  in (2.4) it follows that  $k$  is a function of the aspect ratio  $\alpha$  alone: Fig. 4 presents values of  $k$  varying  $\alpha$ .

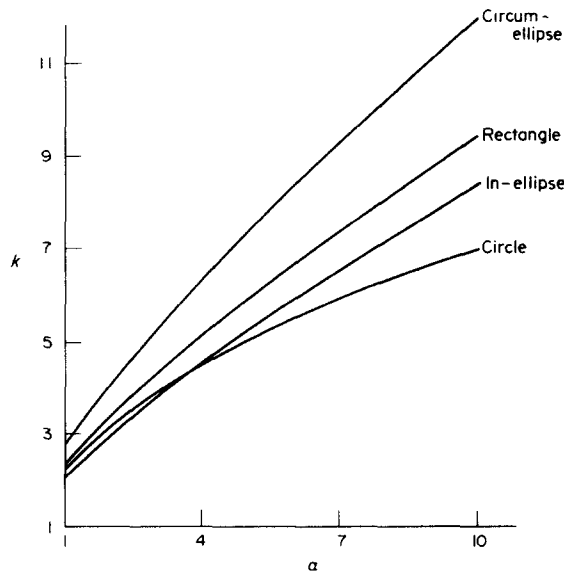


Fig. 4. Stiffness for the lubricated rectangular punch and stiffness bounds.

Although an analytical solution is not available for the lubricated rectangular punch, analytical solutions do exist for the related problems for the circular and elliptical punches‡ and can be used to provide *bounds on the stiffness*. Galin, in [1] Section 2.10, argues that, of all flat punches of equal area, the circular punch has the lowest stiffness (the result stemming from the work of Polya and Szegő[16] on the isomorphic problem of the capacitance of a charged lamina); hence the lower bound marked “circle” in Fig. 4. Two other bounds are furnished by a pair of ellipses: one containing the rectangle—the *circum-ellipse*; the other contained in the rectangle—the *in-ellipse*. Contingent upon the contact stress being of constant sign, these two ellipses provide an upper bound and a further lower bound (see the Appendix for a proof), the latter being superior to the equi-area circle for large aspect ratios. Since the numerical values of the contact stresses are of constant sign we expect their attendant stiffness values to satisfy these bounds and Fig. 4 shows that such is the case.

The analytical solution for the elliptical punch can also be used to provide “equivalent ellipses” in a stiffness sense, one being the ellipse with the same area and aspect ratio. For this ellipse, the stiffness  $k^*$  is given by

$$k^* = 2\alpha\sqrt{\pi}/K(1 - 1/\alpha^2), \quad (\alpha \geq 1), \quad (2.8)$$

where  $K$  is the complete elliptic integral of the first kind, defined by  $K(m) = \int_0^1 [(1-t^2)(1-mt^2)]^{-1/2} dt$ . Values drawn from (2.8) are almost indistinguishable from those for the rectangle on the scale of Fig. 4, differing by a maximum of 2.2% for the range  $(1 \leq \alpha \leq 10)$ .

On comparing the stiffness results found by the method of Gorbunov-Possadov in [4] with

†Full tables of contact stresses and interior stresses are to appear elsewhere.

‡See Lur'e[15], Section 5.

those of Fig. 4, one finds a surprisingly high level of agreement with a maximum discrepancy of 2.6% in the range ( $1 \leq \alpha \leq 10$ ).† Comparison of the result for the stiffness of the square ( $\alpha = 1$ ) given by Conway and Farnham [5] with that of Fig. 4 yields a 3.5% difference—a sufficiently large difference for Conway and Farnham's result to lie below the lower bound in Fig. 4. Finally, comparing the stiffness values at  $\alpha = 5, 10$  obtained by Borodachev and Galin [9] with the corresponding values in Fig. 4 provides the closest agreement yet, with the differences being 1.7% and 1.1% respectively.

We next consider the effects of adhesion.

### 3. THE ADHESIVE RECTANGULAR PUNCH

In this section we analyse the uniform indentation of the elastic half-space by an adhesive rectangular punch. We outline the application of the singularity method and compare the results obtained with the values found for the lubricated case.

The formulation of the problem is identical to that of the lubricated rectangular punch in Section 2, with the exception of the boundary conditions. We now assume the punch to be *adhesive*, or rough, so that no lateral slipping occurs between the punch and the half-space. Accordingly the *boundary conditions* are

$$\begin{aligned} w = d, \quad u = v = 0 \text{ on } \partial_1 \mathcal{H}, \\ \sigma_z = \tau_{yz} = \tau_{zx} = 0 \text{ on } \partial_2 \mathcal{H}, \end{aligned} \quad (3.1)$$

where  $\partial_1 \mathcal{H}$ ,  $\partial_2 \mathcal{H}$  are as defined in (2.1).

The development of the associated *integral equations* for the problem now requires two known solutions: the *Boussinesq solution* for the normal point-load on the elastic half-space, and the *Cerutti solution* for the tangential point-load. On superposing these two solutions, satisfaction of the first of (3.1) leads to the following system of integral equations holding for ( $-a < x < a$ ,  $-b < y < b$ ):

$$\begin{aligned} \frac{1-2\nu}{4\mu\pi} \int_{-b}^b \int_{-a}^a \frac{(x-\xi)p_x(\xi, \eta) + (y-\eta)p_y(\xi, \eta)}{(x-\xi)^2 + (y-\eta)^2} d\xi d\eta + \frac{1-\nu}{2\mu\pi} \int_{-b}^b \int_{-a}^a \frac{p_z(\xi, \eta)}{\sqrt{[(x-\xi)^2 + (y-\eta)^2]}} d\xi d\eta = d, \\ \int_{-b}^b \int_{-a}^a \frac{[(x-\xi)^2 + (1-\nu)(y-\eta)^2]p_x(\xi, \eta) + \nu(x-\xi)(y-\eta)p_y(\xi, \eta)}{[(x-\xi)^2 + (y-\eta)^2]^{3/2}} d\xi d\eta \\ + \frac{1-2\nu}{2} \int_{-b}^b \int_{-a}^a \frac{(x-\xi)p_z(\xi, \eta)}{(x-\xi)^2 + (y-\eta)^2} d\xi d\eta = 0, \end{aligned} \quad (3.2)$$

together with a third equation obtained from the second of (3.2) by interchanging  $(x - \xi)$  with  $(y - \eta)$  and  $p_x$  with  $p_y$ . In (3.2),  $p_x, p_y$  are the *shear contact stresses* and  $p_z$  is the *normal contact stress*, viz.  $p_x = \tau_{zx}$ ,  $p_y = \tau_{yz}$ ,  $p_z = -\sigma_z (= p)$  on  $\partial_1 \mathcal{H}$ .

Notice that on setting  $\nu = 1/2$ ,  $p_x = p_y = 0$  in (3.2), the system of integral equations collapses to the single integral equation of (2.3). Thus the lubricated problem is merely the special case of Poisson's ratio equal to 1/2 in the adhesive problem.

The critical step in the application of the singularity method to (3.2) is the postulation of the character of the *stress singularities*. To this end we consider the related strip problem wherein the contact stresses behave like‡

$$\begin{aligned} \sigma_z = \text{ord } (r^{-1/2} \cos(\kappa \ln r)) \text{ as } r \rightarrow 0, \\ \tau_{zx} = \text{ord } (r^{-1/2} \sin(\kappa \ln r)) \text{ as } r \rightarrow 0, \end{aligned} \quad (3.3)$$

on  $\partial_1 \mathcal{H}$  as defined in (1.2), where  $r$  is once again the distance from either of the punch edges and  $\kappa = (1/2\pi) \ln(3 - 4\nu)$ . We see that, in addition to the square-root singularity, the stresses in (3.3)

†One should bear in mind, however, that close agreement in an average need not reflect a high overall correlation for the contact stress distributions—recall the considerable increases in the error in the second moment of the contact stress distribution cf. the error in the average, in Section 1.

‡See, for example, Muskhelishvili [11], p. 476.

have an anomalous oscillatory nature and undergo infinitely many sign reversals as the edge of the strip is approached. However the region of these oscillations is small, being confined to within  $0.9997a$  of the strip edge (this being the point for the first sign change in the limiting case of  $\nu = 0$ ).† Consequently we take a simplified form of (3.3) and characterize the contact stresses in the rectangular punch by square-root singularities at the edges away from the corners. Further justification for omitting the oscillatory nature in (3.3) can be obtained on applying our singularity method to the adhesive strip with this simplification. When this is done for  $\nu = 0.0, 0.1, \dots 0.5$ , the values found for both  $e_p$  and  $e_m$  support the simplification, being less than 1% for  $N = 3$  and decaying with increasing  $N$  in a similar manner to that found for the lubricated case.

The solution of the wedge problem is not available for the adhesive case. Thus, in the absence of any additional information, we assume the singular nature of the stresses can be accommodated by an inverse-distance singularity as the corners of the rectangle are approached. Such singular behaviour near the corners, in conjunction with that suggested for away from the corners, leads us to take the same form as in Section 2, (2.7), for each of the contact stresses,  $p_x, p_y, p_z$ , in (3.2). As in Section 2, the *regular stresses* so defined are not necessarily “regular” and the choice of these forms awaits numerical vindication.

The numerical results obtained, on the introduction of the forms and the performance of the subsequent routine steps, do in fact support them as estimators of dominant singular character—the regular stress values found having all the hallmarks of a convergent numerical procedure (see [14] for detailed results). We summarize the results by presenting values of the stiffness  $k$ , now a function of the aspect ratio  $\alpha$  and Poisson’s ratio  $\nu$  (Fig. 5).

The effects of adhesion on the stiffness are seen to be small. For the range ( $1 \leq \alpha \leq 10$ ), the greatest increase in the stiffness from that for the smooth case ( $\nu = 0.5$ ) to that for the limiting adhesive case ( $\nu = 0$ ) is 8%; the increases for Poisson’s ratios of 0.2 and 0.3 vary little with  $\alpha$  and average 3.9% and 2.4% respectively.

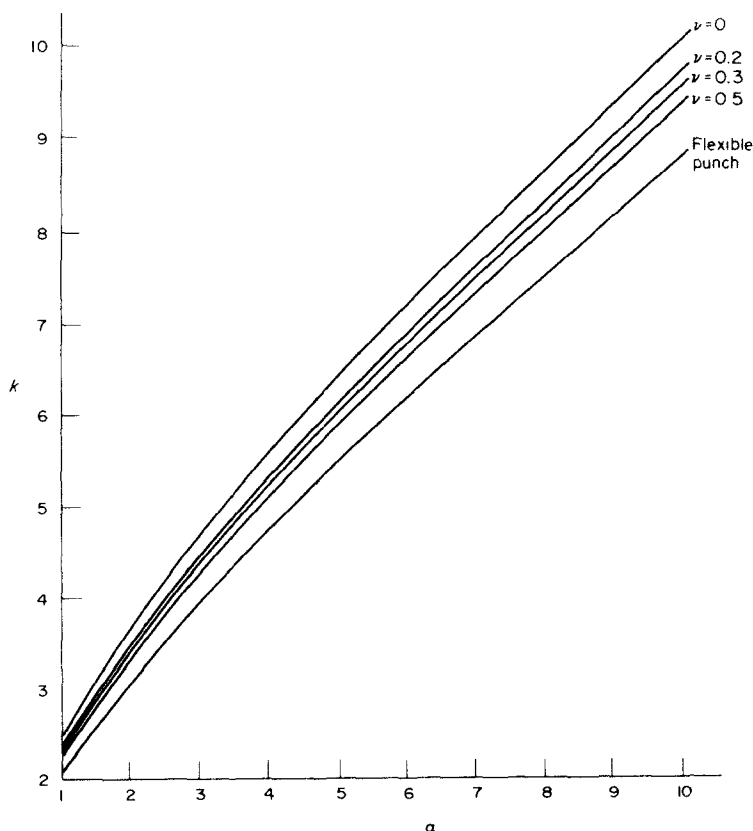


Fig. 5. Stiffness for the rectangular punch with and without adhesion: stiffness for the flexible punch.

†See Muskhelishvili [11], p. 477.

Also presented in Fig. 5, for the purpose of comparison, are the equivalent results for the *flexible punch*, i.e. the case of a constant contact stress throughout the rectangle. In this case the displacement is nonuniform and  $d$  is taken as the average indentation. The stiffness of the flexible punch is from 9% (at  $\alpha = 1$ ) to 6% (at  $\alpha = 10$ ) less than that of the smooth rigid punch.

Finally, and again for the purpose of comparison, we cite the analytical results given by Spence[17] for the stiffness of the *adhesive circular punch*. These are shown in Table 2, together with the results for the adhesive square punch of the same area (the values exhibited are based on the definition of  $k$  in (2.4) wherein  $a$  is the semi-length of the square). For the smooth case ( $\nu = 0.5$ ), the circular punch stiffness is a proven lower bound: it is not proven so for the adhesive case, but nonetheless, for all values of Poisson's ratio examined, the stiffness of the circular punch is about 2% less than that of the square punch.

Table 2. Stiffness values for the adhesive square punch and the adhesive circular punch

Poisson's ratio	0	0.1	0.2	0.3	0.4	0.5
Adhesive square punch	2.52	2.47	2.42	2.37	2.33	2.31
Adhesive circular punch	2.48	2.43	2.37	2.32	2.28	2.26

#### REFERENCES

1. L. A. Galin, *Contact Problems in the Theory of Elasticity*. (English translation by H. Moss and I. N. Sneddon). North Carolina State College translation (1961).
2. J. N. Goodier and P. G. Hodge, *Elasticity and Plasticity*. Wiley, New York (1958).
3. J. L. Lubkin, Contact problems. In *Handbook of Engineering Mechanics* (Edited by W. Flügge). McGraw-Hill, New York (1962).
4. M. I. Gorbunov-Possadov and R. V. Serebrjanyi, Design of structures on elastic foundations. *Proc. Fifth Int. Conf. on Soil Mech. and Foundation Engng* 1, 643 (1961).
5. H. D. Conway and K. A. Farnham, The relationship between load and penetration for a rigid, flat-ended punch of arbitrary cross section. *Int. J. Engng Sci.* 6, 489 (1968).
6. H. D. Conway, S. M. Vogel, K. A. Farnham and S. So, Normal and shearing contact stresses in indented strips and slabs. *Int. J. Engng Sci.* 4, 343 (1966).
7. H. D. Conway and K. A. Farnham, Slabs and shafts compressed by circular indenters. *Int. J. mech. Sci.* 10, 981 (1968).
8. H. D. Conway and P. A. Engel, Contact stresses in slabs due to rough round indenters. *Int. J. mech. Sci.* 11, 709 (1969).
9. N. M. Borodachev and L. A. Galin, Contact problem for a stamp with narrow rectangular base. *Prikl. Mat. Mekh.* 38, 108 (1974).
10. J. K. Knowles and Eli Sternberg, On the singularity induced by certain mixed boundary conditions in linearized and nonlinear elastostatics. *Int. J. Solids Struct.* 11, 1173 (1975).
11. N. I. Muskhelishvili, *Some Basic Problems of the Mathematical Theory of Elasticity*. (English translation by J. R. M. Radok). Noordhoff, Groningen, The Netherlands (1963).
12. A. F. Emery and C. M. Segedin, Singularity programming—a numerical technique for determining the effect of singularities in finite difference solutions illustrated by application to plane elastic problems. *Int. J. Num. Methods in Engng* 6, 367 (1973).
13. V. L. Rvachev, The pressure on an elastic half-space of a stamp with wedge-shaped planform. *Prikl. Mat. Mekh.* 23, 229 (1959).
14. P. W. Brothers, The rigid rectangular punch on the elastic half-space. M.E. thesis, University of Auckland, Auckland, New Zealand (1976).
15. A. I. Lur'e, *Three-Dimensional Problems of the Theory of Elasticity*. (English translation by D. B. McVean and J. M. Radok). Interscience, New York (1964).
16. G. Polya and G. Szegő, Inequalities for the capacity of a condenser. *Amer. J. Math.* 67, 1 (1945).
17. D. A. Spence, Self similar solutions to adhesive contact problems with incremental loading. *Proc. R. Soc. A* 305, 55 (1968).

#### APPENDIX

##### *Derivation of upper and lower bounds for the stiffness of the lubricated rectangular punch*

Here we sketch a derivation of the bounds on the rectangular punch stiffness furnished by a pair of elliptical punches (refer Fig. 4, Section 2). In order to state these bounds concisely and to minimize explanation of the notation used, we adopt the following convention: unprimed quantities are associated with the rectangle, quantities with a single prime are associated with the in-ellipse, and those with a double prime with the circum-ellipse. Thus a statement of the bounds can be made as follows: if (i) all three punches rest on the same half-space  $\mathcal{X}$  and share a common depth of uniform indentation  $d$ ; and (ii) the contact stress for the rectangle is nowhere negative (i.e.  $p \geq 0$  on  $\partial_1 \mathcal{X}$ ): then

$$(a'/a)k' \leq k \leq (a''/a)k'', \quad (1)$$

where  $a'$ ,  $a''$  are the  $x$ -intercepts of the in-, circum-ellipses.

To prove (1) we first observe that, from the definition of the stiffness in (2.4) with " $a$ " suitably replaced therein with  $a'$ ,  $a''$ , and under (i), (1) is equivalent to

$$P' \leq P \leq P''. \quad (2)$$

Hence we seek to show (2) holds.

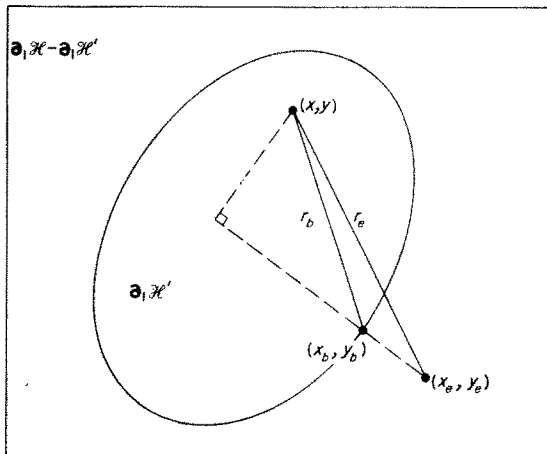


Fig. 6. Contact regions for the in-ellipse and rectangle.

To this end, note that the loadings in all three problems can be constructed by the superposition of point-loads over bounded regions. Consequently their stresses are  $O(r^{-2})$  and their displacements  $O(r^{-1})$  as  $r \rightarrow \infty$ , where  $r$  is now the distance from the origin 0. Subject to this decay at infinity, the extension of Betti's reciprocal theorem to the infinite region  $\mathcal{K}$  is elementary. We now apply Betti's theorem on  $\mathcal{K}$  to the punch problems implicit in (2).

We begin by considering the in-ellipse and the rectangle. For this pair, Betti's theorem gives

$$\int_{\partial_1 \mathcal{K}'} w p' dA = \int_{\partial_1 \mathcal{K}} w' p dA, \tag{3}$$

where  $dA$  indicates integration over the contact surfaces and we have used the fact that the surface of  $\mathcal{K}$  is stress free outside outside the punches. Introducing the displacements under the punches, (3) becomes

$$d \int_{\partial_1 \mathcal{K}'} p' dA = d \int_{\partial_1 \mathcal{K}} p dA + \int_{\partial_1 \mathcal{K} - \partial_1 \mathcal{K}'} (w' - d) p dA,$$

or

$$P - P' = I, \quad I = \frac{1}{d} \int_{\partial_1 \mathcal{K} - \partial_1 \mathcal{K}'} (d - w') p dA. \tag{4}$$

It therefore remains to show  $I \geq 0$  to establish the first inequality in (2); or, since  $d$  and  $p$  are positive on  $\partial_1 \mathcal{K} - \partial_1 \mathcal{K}'$  (by (ii)), to show that  $d \geq w'$  on  $\partial_1 \mathcal{K} - \partial_1 \mathcal{K}'$ .

Let  $(x_e, y_e)$  be any point on  $\partial_1 \mathcal{K} - \partial_1 \mathcal{K}'$  and  $(x_b, y_b)$  the point on the boundary closest to  $(x_e, y_e)$ ; because  $\partial_1 \mathcal{K}'$  is an ellipse and is therefore convex,  $(x_b, y_b)$  is unique for any  $(x_e, y_e)$ . Let  $(x, y)$  be any point inside  $\partial_1 \mathcal{K}'$  and let  $r_b$  be the distance between  $(x, y)$  and  $(x_b, y_b)$  with  $r_e$  the distance between  $(x, y)$  and  $(x_e, y_e)$  (Fig. 6).

Now  $r_b \leq r_e$  (by Pythagoras) so that

$$\int_{\partial_1 \mathcal{K}'} \frac{p'}{r_b} dA \geq \int_{\partial_1 \mathcal{K}'} \frac{p'}{r_e} dA. \tag{5}$$

Hence  $d \geq w'$  for any point on  $\partial_1 \mathcal{K} - \partial_1 \mathcal{K}'$  and the first inequality in (2) holds.

Turning to the second inequality in (2), observe that the foregoing argument is valid for any pair of nested contact regions provided that the inner region is convex and that the contact stress associated with the outer region is nowhere negative. Thus, since a rectangle is convex and the contact stress for the ellipse is positive, the last inequality in (2) follows immediately.

The actual bounds shown in Fig. 4, Section 2, stem from particular choices of the in- and circum-ellipses. The in-ellipse taken is the ellipse touching the four mid-points of the rectangle sides, this being the ellipse which maximizes the lower bound in (1). The circum-ellipse taken is the ellipse with the same aspect ratio as the rectangle and which passes through all four corners; while this is not the ellipse which minimizes the upper bound in (1), it differs by a negligible amount from the minimum and is computationally convenient.